Electrochimica Acta 421 (2022) 140476

Contents lists available at ScienceDirect

Electrochimica Acta

journal homepage: www.journals.elsevier.com/electrochimica-acta

Effects of ethylenediamine tetrakis(ethoxylate-block-propoxylate) tetrol on tin electrodeposition

Y. Hu [a], K. Ahammed [a], Q. Liu [a], R. Williams [a,b], Q. Huang [a,*]

[a] Department of Chemical and Biological Engineering, The University of Alabama, Tuscaloosa, AL 30487, United States
[b] Department of Electrical and Computer Engineering, Mississippi State University, Starkville, MS 39759, United States

ARTICLE INFO

Keywords:
Electrodeposition
Tin
Organic additive
Through silicon via
Suppression

ABSTRACT

Electrodeposition of Tin (Sn) is studied in the presence of ethylenediamine tetrakis(ethoxylate-block-propoxylate) tetrol (ETT). Cyclic voltammetry (CV), chronoamperometry, and chronopotentiometry are conducted to characterize the electrochemical behavior of Sn with the addition of ETT. Several influencing factors such as the ETT concentration, rotation rate, and potential scan rate are systematically investigated, and it is found that ETT suppresses Sn deposition at a certain negative potential range due to a potential dependent adsorption of ETT. This adsorption of ETT is further dependent not only on the empty surface fraction but also the occupied fraction or surface coverage. Moreover, various additives containing different functional groups of ETT are used to determine the key structural component for the inhibition effect.

1. Introduction

Tin (Sn) is widely used to establish electrical connections in the electronic devices because it not only offers protection for the base metal from oxidation [1–3] but also ensures solderability of the base metal [4, 5]. Electrolytes based on stannous sulfate are commonly used for Sn electrodeposition in the electronic industry and organic additives are often added to prevent the formation of needles, whiskers, and dendrites on Sn films [6–14]. Three different kinds of additives classified as surfactants, oxidation inhibitors, and grain refiners are often added to plating baths to control the film morphology, brightness, and grain refinement, respectively [15]. Surfactants are added to promote the polarization of electrode reactions. There are extensive studies on surfactants for Sn deposition and several types of chemicals, such as glycol additives [8], alkyl carbonyl compounds [11], and aromatic carbonyl compounds [16], have been reported to show suppression effects on Sn deposition. The suppression effect is found to relate to the adsorption of additives on Sn surface, which blocks the active sites on substrate and slows down the charge transfer, resulting in an increased overpotential for Sn deposition [11]. Oxidation inhibitors are used to suppress the formation of stannic ions in the electrolyte and reduce the sludge precipitation. Common antioxidants include hydrazine, carbohydrazide, hydroquinone, and diethylhydroxylamine [15]. Grain refiners are typically added to produce smooth or bright Sn films [11,17]. There are some overlaps between surfactants and grain refiners. For example, the presence of a combination of Synthanol DS-10, formalin, and benzyl alcohol in the Sn sulfate electrolyte not only suppresses Sn deposition but also reduces roughness of Sn film [17]. These additional chemicals are essential for producing Sn films with enhanced properties and morphology required for electronic and other applications.

The electrodeposition of copper and a few other transition metals in through silicon vias (TSV) is commonly carried out with multiple additives (accelerator, suppressor, and leveler), which selectively suppress and accelerate the deposition rate to enable super-conformal or bottom-up filling [18–25]. Recently, many studies have been conducted to explore single additive systems [26–35], where suppressors such as polyether are found to be effective in enabling bottom-up metal filling. Different techniques, including electrochemical analysis [28,33,36,37], *in situ* ellipsometry [38], surface enhanced Raman spectroscopy [39], and surface enhanced infrared absorption spectroscopy[40], have been employed to demonstrate that polyether adsorbates form an effective layer on the surface, restricting access of Cu^{2+} to the electrode surface and thus inhibiting Cu deposition. The effects of polyether suppressors have been reported for the electrodeposition of various transition metals including gold [41,42], zinc [43], nickel (Ni) [44,45], cobalt [46], and copper (Cu) [26–35] and defect-free TSV fillings with these metals can be successfully achieved in the presence of polyether suppressors. In an attempt to form superconducting TSVs for integrated quantum circuits,

* Corresponding author.
E-mail address: qhuang@eng.ua.edu (Q. Huang).

https://doi.org/10.1016/j.electacta.2022.140476
Received 9 February 2022; Received in revised form 23 March 2022; Accepted 29 April 2022
Available online 1 May 2022

the same super-conformal filling would be needed for superconducting materials. Sn is a well-known superconductor with a superconducting transition temperature or a critical temperature of 3.7 K [47]. However, studies are very limited on the suppressors for Sn electrodeposition needed for the filling.

This paper presents a study of the effects of ethylenediamine tetrakis (ethoxylate-block-propoxylate) tetrol (ETT, commercial name Tetronic 90R4, average MW 7,200), a molecule with four polyether block co-polymers connecting together through an ethylenediamine, on Sn electrodeposition. This type of additive, albeit with a different molecular weight, has been previously shown to successfully enable Cu bottom up filling in extremely high aspect ratio TSVs [37,48,49]. Here, a systematic study is carried out not only to characterize and understand the suppression mechanism of ETT on Sn deposition but also to dissect the effects of different structural components of ETT on this inhibition effect.

2. Experimental

A traditional three-compartment electrochemical cell is used for the experimental studies. The counter electrode is a 99.99% Pt foil placed in the anolyte compartment separated from the catholyte by a glass frit. A saturated Ag/AgCl electrode (0.197 V vs. SHE) is used as the reference electrode, and all potentials are referred to this electrode. The reference electrode compartment is connected to the catholyte through a capillary. Pt rotating disk electrode (RDE, 0.196 cm^2) is used as the working electrode. Pt RDE is anodically stripped and chemically cleaned with nitric acid after each deposition.

The Sn makeup solution contains 0.15 M $SnSO_4$ and 1 M H_2SO_4. It is freshly prepared before each use and there is no sludge precipitation in the solution. Different additives including N,N,N',N'-Tetrakis (2-hydroxypropyl) ethylenediamine (99%, MW 292.4), N,N,N',N'-Tetrakis (2-hydroxyethyl) ethylenediamine (99%, MW 236.3), Ethylenediamine (99%, MW 60.1), Poly(propylene glycol) (PPG, average MW 4,000), Polyethylene glycol (PEG, average MW 4,000), Poly(ethylene glycol)-block-poly(propylene glycol)-block-poly(ethylene glycol) (PEG-PPG-PEG, average MW 4,400), and ETT (average MW 7,200) are dissolved in water to prepare the additive stock solutions with a fixed concentration of 60,000 ppm. Because the cloud point of PEG-PPG-PEG (14°C) is lower than room temperature (20°C), this particular stock solution is stored in an ice cooler to ensure homogeneity and stability. The small amount of stock solution used in experiments does not have any significant impact on the overall temperature of experiment and the additive remains completely soluble at the final concentrations used in electrolyte. Calculated amounts of additives are then added into the Sn make up solutions up to various final concentrations. All salts are at least ACS grade and used as received. All organic additives are acquired with the above listed specifications and are also used as received. Deionized (DI) water with a resistivity of 18.2 MOhm-cm is used in all studies.

An Autolab 302N potentiostat is used for all electrochemical studies. The effects of additive on Sn deposition are studied using cyclic voltammetry, chronoamperometry and chronopotentiometry. Among them, the non-steady state transient behavior of additives is studied using choropotentiometry, where additives are injected at the vicinity of RDE using a pipette. A layer of Sn is pre-plated on Pt RDE using the Sn make up electrolyte (additive free) at -40 mA/cm^2 for 30s at a fixed rotation rate of 500 rpm.

3. Results and discussion

3.1. Suppression mechanism of ETT

Fig. 1 shows the cyclic voltammetry (CV) of Sn electrodeposition on Sn-preplated Pt RDE at two different conditions, where a suppression effect of ETT is observed. The electrolyte comprises 0.15 M $SnSO_4$, the rotation rate is 1000 rpm, and the scan rate is 20 mV/s. Sn deposition in absence of additives starts at around -0.43 V, and the current density

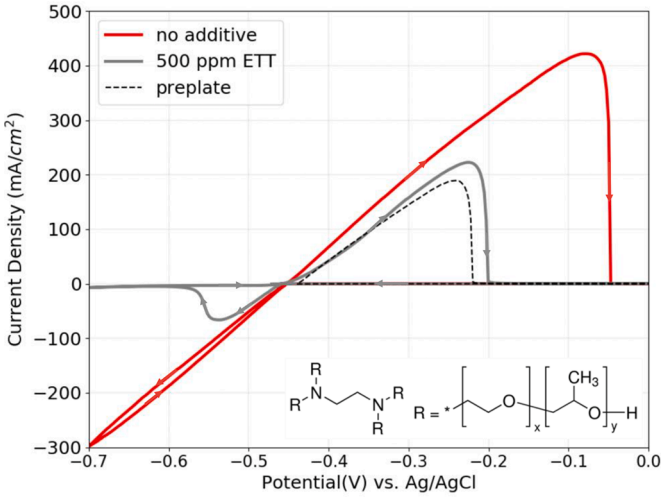

Fig. 1. Cyclic voltammetry of Sn electrodeposition on Sn-preplated Pt RDE at 1000 rpm in 0.15 M Sn solutions with and without ETT. Scan rate = 20 mV/s. Inset in the figure shows the molecular structure of ETT.

increases as the potential becomes more negative. Adding 500 ppm ETT into the electrolyte results in an inhibition for Sn deposition. The deposition starts at the same potential of -0.43 V, indicative of the same reversible potential of Sn. The magnitude of current density increases as potential decreases in the same way as additive free solution at the beginning. However, as the potential continues to decrease, the current density drops and reaches nearly zero at more negative potentials, thus resulting in a cathodic current peak. For the backward scan, the current density remains at nearly zero for the entire cathodic range creating a hysteresis loop in the cathodic potential range. In the anodic regime, the stripping current reflects how much Sn is deposited during the cathodic sweeps. The stripping of pre-plated Sn on Pt RDE is also presented for comparison. The area differences among three anodic stripping peaks confirms that the Sn deposition is significantly inhibited with the addition of 500 ppm ETT. While systematic film characterization will be presented elsewhere, a quick comparison of the film morphology of Sn deposited in absence ETT and in presence of 500 ppm ETT is presented in Fig. S-1 in the Supporting Information. Sn films deposited additive free are not coalescent even after a 5-μm equivalent film thickness. Huge crystals are deposited with size up to 50 μm at -5 mA/cm^2. This max crystal size decreases slightly to 25 μm at a higher deposition current of -20 mA/cm^2. On the other hand, films are completely continuous when 500 ppm ETT is used. Topographical features between 1 to 10 μm in size are observed depending on the deposition current. This grain refining effect is consistent with the expectation for a suppressing surface adsorbate, where the adsorption preferably occurs on Sn surface hindering the further growth of Sn nuclei but promoting the formation of new nuclei on the substrate.

Fig. 2 shows the CV results at different concentrations of ETT. They are separated into two panels with two different concentration ranges (lower ones in 2(a) and higher in 2(b)). As shown in Fig. 2(a), a minor suppression effect is observed with the addition of 40 ppm ETT. The current density curve nearly follows the additive free case except for a kink at about -0.52 to -0.55 V, which results from a weak suppression effect but quickly disappears at potentials more negative than -0.55 V. Increasing ETT concentration to 60 ppm further suppresses the Sn deposition. The current density initially follows the same trend as the 40 ppm, but it keeps decreasing to nearly -10 mA/cm^2 at around -0.60 V. Afterwards, the current density starts to gradually increase until the lower potential vertex of -0.7 V is reached. On the backward scan, the deposition current also decreases at -0.60 V and stays low for the entire cathodic regime before the anodic stripping. Fig. 2(b) shows the same CV studies with 80 to 500 ppm ETT. When 80 ppm ETT is added into the

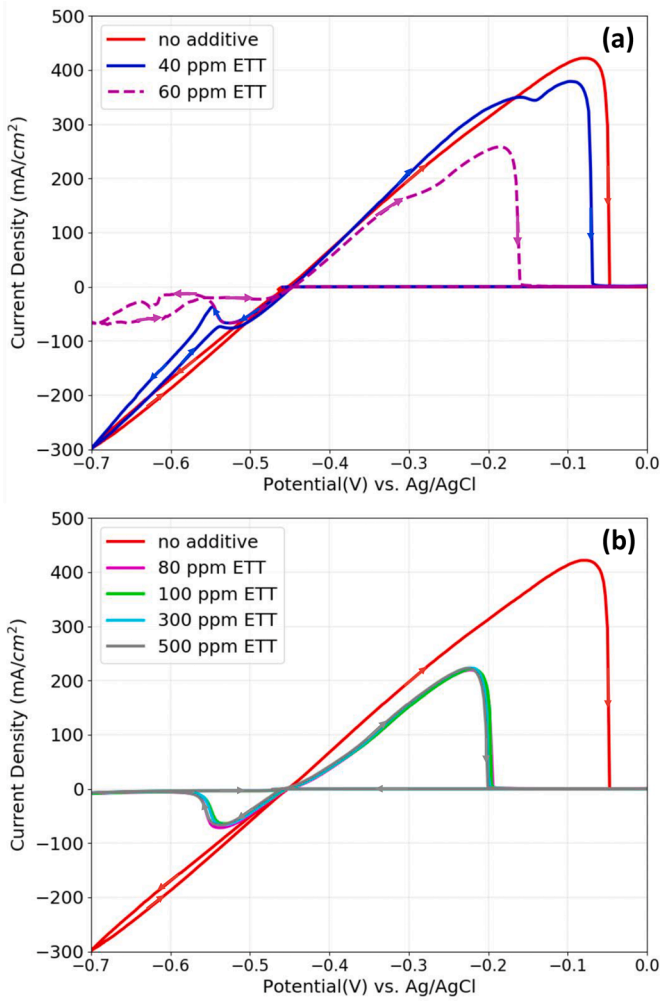

Fig. 2. Cyclic voltammetry of Sn electrodeposition at 20 mV/s on Pt RDE at 1000 rpm in 0.15 M Sn solutions with (a) 0, 40, 60 ppm ETT and (b) 0, 80, 100, 300, 500 ppm ETT.

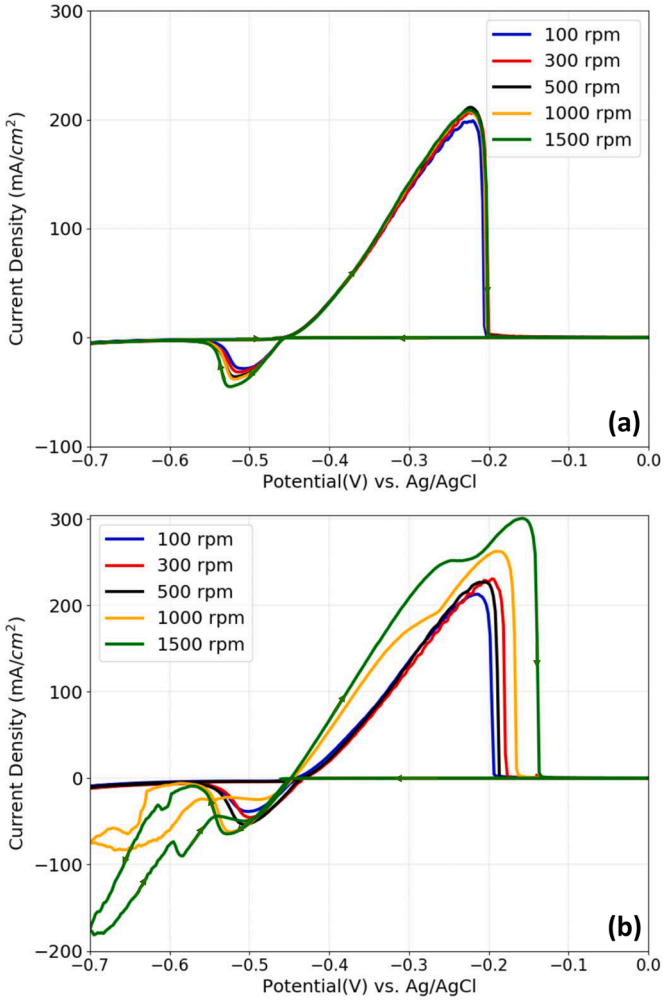

Fig. 3. Cyclic voltammetry of Sn electrodeposition at 20 mV/s on Pt RDE in 0.15 M Sn solutions at different rotation rates with (a) 500 ppm ETT; (b) 60 ppm ETT.

solution, a stronger suppression effect on Sn deposition is observed, where current density falls to nearly 0 mA/cm^2 as the potential is more negative than -0.58 V and it remains at nearly zero in the backward scan. No significant change can be observed when more ETT are added into the electrolyte, indicating that the suppression effect of ETT is saturated.

To summarize the results, several interesting phenomena are observed in the Sn deposition with ETT: (i) The OCP of Sn deposition is not changed with the addition of ETT; (ii) The suppression effect of ETT emerges at relative more negative potentials; (iii) A breakdown of suppression effect can occur at even more negative potentials, but only at low ETT concentrations; (iv) The suppression effect is saturated with 80 ppm or more ETT for the conditions studied.

One thing to note is that the above observations are based on current measurements. A separate set of deposition and stripping studies are carried out (not shown here) and the current efficiency of Sn deposition across all different conditions used in this report, that is regardless of ETT concentration and current densities, is nearly 100%. Therefore, the side reaction is negligible during Sn deposition, consistent with the low exchange current of HER on Sn surface, and the observed current change is nearly 100% reflective of the Sn deposition rate.

Fig. 3(a) shows the effect of rotation rates on Sn deposition with 500 ppm ETT. It is interesting that the height and area of current peaks slightly increase as the rotation rate increases. In other words, the suppression effect of ETT is slightly alleviated at high rotation rates. As discussed earlier, the suppression effect of ETT on Sn deposition results from the adsorbed ETT blocking Sn surface. Therefore, it is possible that the adsorbed ETT is swept away by hydrodynamic shear stress at higher rotation rates, slightly easing the charge transfer for Sn deposition. On the other hand, while the adsorption rate and suppression effect of ETT are also expected to relate to its surface concentration, the high concentration of 500 ppm used here is known (Fig. 2) more than enough to saturate the surface adsorption. To further investigate the effects of rotation rate, 60 ppm ETT, which is barely below the saturation concentration, is used and the results are shown in Fig. 3(b). First at a rotation rate of 500 rpm or below, a typical Sn deposition behavior with saturated suppression effect is observed, i.e., the height of current peak only slightly increases as the rotation rate increases, similar to Fig. 3(a). However, a higher rotation rate of 1000 rpm results in the breakdown of suppression effect at around -0.62V. This also confirms the reproducibility of the results observed earlier in Fig. 2(a) at the same concentration of 60 ppm. Consequently, the anodic peak at 1000 rpm is significantly larger than at lower rotation rates (100, 300, 500 rpm) because more Sn has been deposited. Further increasing the rotation rate to 1500 rpm leads to an earlier breakdown of suppression effect, at -0.56 V, and a larger anodic stripping peak.

This result clearly illustrates the role of rotation rate or agitation in Sn deposition with ETT. When the agitation is mild, i.e., at a rotation rate of 500 rpm or below, the detachment of adsorbed ETT upon the hydrodynamic shear force is slow and can be easily cancelled out by the adsorption of ETT from electrolyte. In this case, the suppression effect

sustains. However, under strong agitation, or at a rotation rate of 1000 rpm or above, this equilibrium is disrupted, the ETT surface coverage decreases, and a suppression breakdown is observed. The threshold agitation, between 500 to 1000 rpm in this case, is dependent on the adsorption rate and the bulk concentration of ETT. At a high concentration of 500 ppm, such breakdown is not observed even at a 1500 rpm rotation rate.

It has been reported that ETT can be used as a poloxamer suppressor in Cu TSV filling process [40,48,50,51]. The proposed mechanism for the suppression effect on Cu is that the polymer and Cl^- strongly co-adsorb on the substrate surface and the blocking halide-poloxamer layer inhibits Cu deposition by restricting access of Cu^{2+} to the free substrate surface. A potential dependent adsorption and a current dependent consumption result in a so called negative differential resistance, which enables a binary deposition behavior. Namely, Cu deposition is completely suppressed at the top and side walls of TSV whilst rapid Cu deposition occurs almost exclusively at the bottom, i.e., bottom-up filling. During such deposition, a minimum agitation is often beneficial for such filling as it mainly minimizes the mass transport and helps to maintain an unsuppressed deposition at the growth front. Here in this study on Sn, the adsorption appears much weaker (in absence of halides). A stronger agitation does not promote the suppression by supplying additive molecules, but rather, it weakens the suppression by mechanically detaching the adsorbate.

Fig. 4 shows the effects of scan rate on the Sn deposition with 500 ppm ETT. The general behavior of Sn deposition with a cathodic current peak is observed for all cases. However, as the scan rate increases, the height of current peak increases and the peak position shifts to more negative potentials. The cathodic peak current and the two charges calculated from cathodic deposition and anodic stripping are listed in the Table 1. First, the difference between these two charges remains roughly as a constant, about 1140 mC/cm^2, consistent with a Sn layer pre-plated on Pt RDE at -30 mA/cm^2 for 40 s with a Faraday efficiency close to 100%. Second, the time from OCP to the cathodic current peak are also listed in Table 1. While the peak position shifts to more negative potentials as scan rate increases, it indeed takes less time to reach the peak current, or in other words, the suppression effect emerges sooner. This raises the question how ETT adsorbs on the Sn surface, or what is the key factor that changes the amount of ETT on electrode surface. Potential dependent suppression is not uncommon in metal deposition including Sn. For example, surface enhanced Raman spectroscopy showed that the long hydrophilic tail in the Triton X-100 would adsorb onto Sn electrode surface and block the deposition more effectively when the potential is around -0.50 V [8]. However, should a single

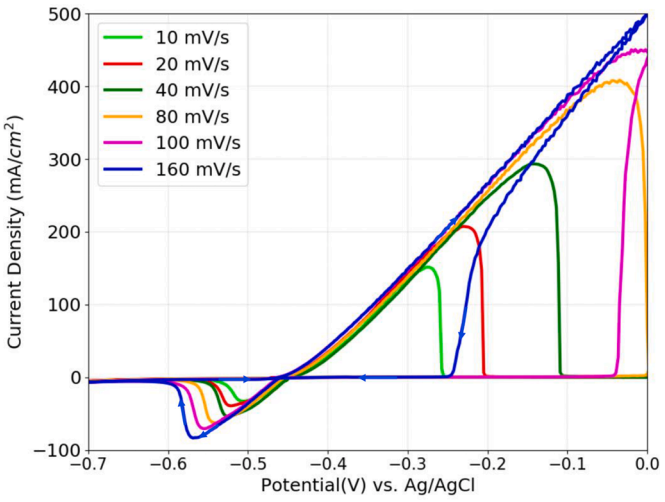

Fig. 4. Cyclic voltammetry of Sn electrodeposition at 20 mV/s on Pt RDE at 1000 rpm in 0.15 M Sn solutions and 500 ppm ETT at different scan rates.

Table 1
The charges and cathodic peak current at different scan rates obtained from the potential transients shown in Fig. 4.

Scan Rate (mV/s)	Cathodic peak current density (mA/cm^2)	Deposition charge density (mC/cm^2)	Stripping charge density (mC/cm^2)	Cathodic peak position (mV)	Time to reach peak current (s)
10	-33.04	-302.5	1440.8	-506	5.19
20	-39.35	-164.7	1331.8	-522	3.08
40	-54.00	-116.7	1291.0	-524	1.87
80	-62.59	-68.3	1229.9	-542	1.08
100	-70.72	-64.6	1200.0	-554	0.91
160	-83.61	-48.8	1169.7	-569	0.67

adsorption potential also apply to ETT here, then the cathodic current would have peaked at a same potential and the time delay from OCP to the peak would have been inversely proportional to the scan rate. This is not the case as shown in Table 1. Therefore, it is hypothesized that the adsorption rate of ETT is positively correlated with the applied cathodic potential. In other words, ETT adsorbs on Sn surface more rapidly at more negative potentials, expediting the suppression effect.

In order to further confirm the potential dependency and time dependency of ETT adsorption on Sn surface, the same CV studies are conducted with additional potentiostatic pre-treatment. The Sn-preplated Pt RDE is first biased at different potentials ranging from OCP to -0.60 V for 30 s in a Sn solution with 500 ppm ETT, immediately after which the same CV studies are performed in the same solution. Fig. 5(a) shows the current transients during the pre-treatment at different potentials. When OCP is applied, the current density maintains at 0 mA/cm^2 as expected. As potential is increased to -0.45 V, the current density slightly increases along the time and reaches -5 mA/cm^2 after 30 sec. A S-shape curve is observed when -0.50V is applied. The change of current density can be interpreted as three different stages. In the initial stage, the magnitude of current density slowly decreases from -28 mA/cm^2 to -25 mA/cm^2. In the middle stage, the current density rapidly drops from -25 mA/cm^2 to around -10 mA/cm^2. In the final stage, the decrease of current density slows down and the current density stabilizes at -5 mA/cm^2. When the pre-treatment potential is adjusted to -0.55 V, the time for initial stage and middle stage significantly decrease. The current density drops from -32 mA/cm^2 to -4 mA/cm^2 within around 4 s and stays at -4 mA/cm^2 for the rest of time. Decreasing the potential to -0.60 V further accelerates the current drop. The initial stage and middle stage become so short that it only takes less than 1 s for the current density to decrease from -33 mA/cm^2 to -4 mA/cm^2. Similar to -0.55V case, the current maintains around -4 mA/cm^2 for the rest of deposition time. Based on the proposed mechanism, these three stages in the current transient are believed to reflect the different stages of ETT adsorption or different surface coverage.

For a typical Langmuir isotherm adsorption with a fixed chemical concentration, the adsorption rate solely depends on the empty surface fraction and the desorption solely on the occupied fraction or surface coverage. As a result, the surface coverage increases following an exponential relationship with time and reaching a saturation value determined by the adsorption and desorption equilibrium. However, the S-shaped current decay observed here is different from an exponential decay, suggesting that the increase rate of the effective ETT surface coverage, or the ETT adsorption rate, positively correlates to not only the empty surface site but also the occupied surface fraction. For example, when desorption is negligible, a simple mathematical representation below can be used to describe the positive correlation between the adsorption rate and the surface coverage, θ, and empty surface fractions, $1-\theta$,

$$\frac{d\theta}{dt} = k\cdot\theta^m\cdot(1-\theta)^n \quad (1)$$

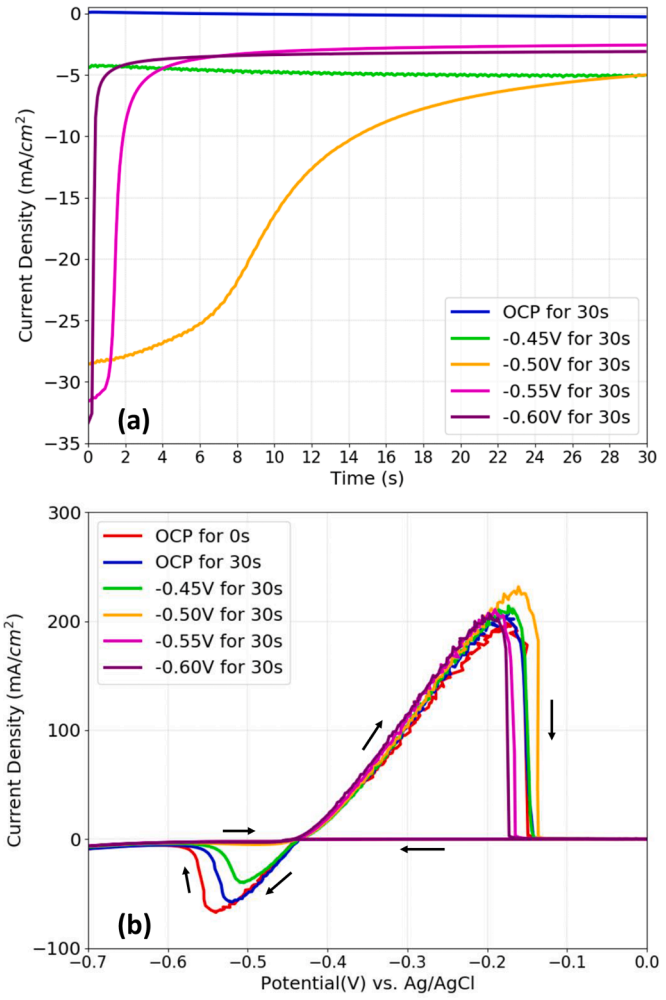

Fig. 5. (a) Current density-time transients for Sn deposition on Sn-preplated Pt RDE at different potentials in 0.15M Sn solutions with 500 ppm ETT; (b) Cyclic voltammetry (scan rate 20 mV/s) of Sn electrodeposition after pre-treatment at different potentials. RDE rotation rate is 1000 rpm.

where θ is the surface coverage, t is time, k is the adsorption constant, m and n are the power dependencies on the occupied and empty surface fractions, respectively. For a special case where the adsorption only depends on empty surface cites by first order, namely $n = 1$ and $m = 0$, the integrated surface coverage θ would follow an exponential relation with time. Here, m and n are two positive numbers, resulting in the S-shaped $\theta - t$ relationship. The fact that the S-shape in Fig. 5(a) is asymmetrical suggests m and n are not equal. It is well understood and expected that the adsorption rate is related to empty surface fraction, but the dependence on the occupied surface fraction is rather unexpected. One hypothesis could be that adsorption is enabled or facilitated by the attractive interaction between ETT molecules adsorbed on surface and ETT molecules in solution. An exemplary plot of θ with respect to t is provided as Fig. S-2 in the Supporting Information for illustration purpose, where k values are adjusted so that the θ curves approximately match the current profiles at -0.5, -0.55, and -0.6 V in Fig. 5(a). The different rates of current decay at different potentials clearly suggest that the adsorption rate constant k is potential dependent.

Fig. 5(b) shows CV studies following the potentiostatic treatment. The OCP remains the same, around -0.44 V, regardless of the potentiostatic pretreatment and it is used as the starting potentials of CV studies. The same CV scan without potentiostatic treatment is also included for comparison and it is labeled as "OCP for 0 s". The comparison between "OCP for 0 s" and "OCP for 30 s" cases shows that Sn deposition is suppressed even no current was applied during the pretreatment. In other words, ETT adsorbs onto the Sn surface even without external bias. The deposition is further suppressed when -0.45V was applied for 30s. When the electrode is pretreated with a potential more negative than -0.50V, immediate suppression is observed in the following CV study, where the CV curves are almost flat and the current density remains very low at -5 mA/cm^2 for the entire cathodic range. In this experiment, no threshold potential is observed for the pretreatment step in terms of bringing about the subsequent suppression effect in CV. The current transient results during the potentiostatic treatment and the different suppression effects observed in the following CV studies are both consistent with the hypothesized theory that the adsorption rate of ETT is positively related to the potential. The more negative potential used in the pretreatment, the faster ETT adsorbs, the faster current decays in the pretreatment, and the earlier and/or stronger suppression effect in the subsequent CV study.

This proposed potential dependent adsorption mechanism is further confirmed with a prolonged pretreatment at a less negative potential, which is shown in Fig. S-3 in Supporting Information. The immediate and complete suppression with a flat current curve, same as the case of -0.50 V in Fig. 5(b), is also observed with a 300 s pre-treatment at -0.45 V. While the adsorption rate constant at -0.45 V can be low, a much longer treatment eventually allows a full surface coverage when the desorption is negligible.

3.2. *Effect of functional groups of ETT*

Functional groups play an important role in determining the behavior of chemicals. In this study, a number of additives are selected to explore the influence of specific structural components of ETT on the inhibition of the Sn deposition. The chemicals examined, which are shown in Fig. 6, include linear PEG, PPG, and triblock PEG-PPG-PEG block copolymer, as well as some other chemicals with the same ethylenediamine core structure, such as N,N,N',N'-Tetrakis (2-Hydroxypropyl) ethylenediamine.

Fig. 7 shows the CV studies of different additives on Sn deposition. While the molecular weights of different molecules are different, a high mass concentration of 500 ppm in conjunction with 1000 rpm rotation rate is used across all different molecules in this study. Molar concentration of the additives are also provided in the caption, where the 500 ppm ETT is of the lowest value. Because the combined atomic weights of -CH_2-, -NH- and -O- groups are similar, a same mass concentration (500 ppm) reflects a similar molar concentration of such structural groups. From previous discussion, this concentration is much higher than the critical concentration (80 ppm for ETT) to saturate the suppression. Therefore, it is believed that this study provides a valid comparison of the suppression effect among different additives when additive depletion is not of a concern. Fig. 7(a) presents the effects of three different non-polymer derivatives of ethylenediamine. In comparison with the additive free case, none of these three chemicals suppresses Sn deposition. From the perspective of molecular structure, this proves that the suppression effect of ETT cannot be solely attributed to the amine groups or ethylenediamine. In other words, when the ethylene diamine structure is only associated with small hydrophilic groups, no suppression can be observed. In Fig. 7(b), 500 ppm of four different polymer additives including ETT are examined, and various levels of suppression effect are observed. When 500 ppm PEG is added to the solution, the deposition is not suppressed until the potential is more negative than -0.58V. The current density maintained at a plateau around -120 mA/cm^2 for the entire potential range beyond -0.58V. The backward scan almost identically traces back the forward scan and the deposition current gradually decreases when the potential becomes more positive than -0.58V. When 500 ppm PPG is added into the electrolyte, a weak suppression effect can be seen immediately at the beginning of deposition or at less negative potentials. Similar to the 40 ppm ETT case in Fig. 2(a), the decrease of current stops at around -0.55V and the current

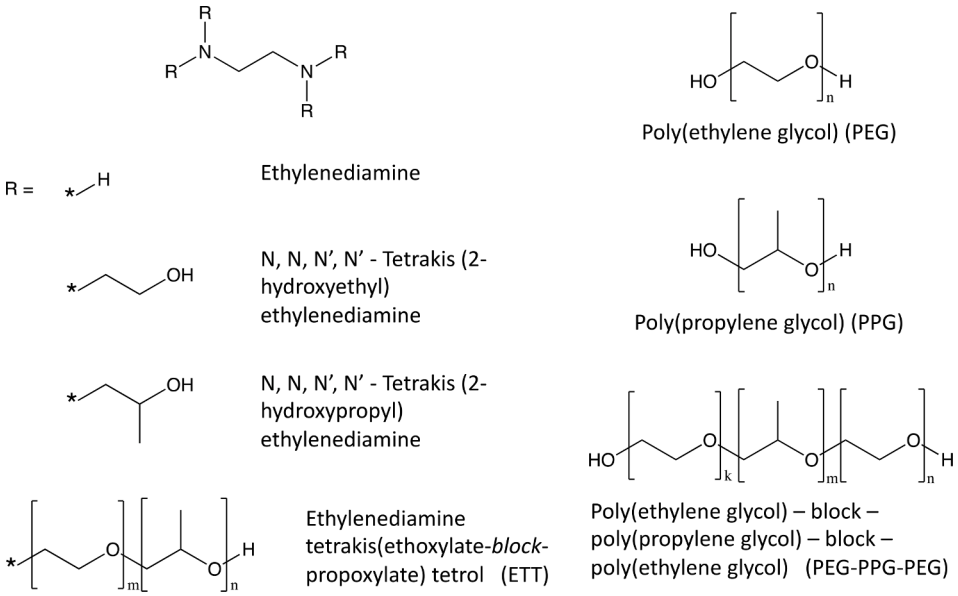

Fig. 6. Molecular structures of additives various functional groups of ETT.

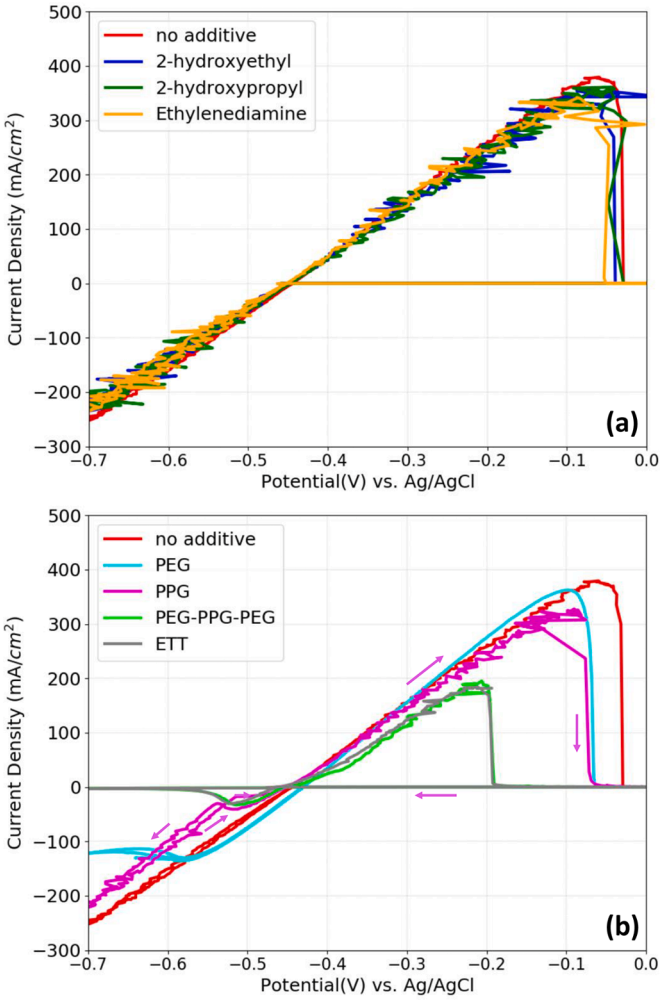

Fig. 7. Cyclic voltammetry of Sn electrodeposition on Pt RDE at 1000 rpm in 0.15 M Sn solutions with 500 ppm (a) Tetrakis(2-hydroxyethyl) ethylenediamine (2.1 mM), Tetrakis(2-hydroxypropyl) ethylenediamine (1.7 mM), and Ethylenediamine (8.3 mM) (b) PEG (0.13 mM), PPG (0.13 mM), PEG-PPG-PEG (0.11 mM), and ETT (0.07 mM).

density starts to increase again as the potential becomes more negative. The suppression effect of PPG and PEG on Sn deposition has been previously reported in methanesulfonate electrolyte system [8], where only a mild suppression effect of PEG was observed and was attributed to the weak adsorption on Sn surface. This seems to be consistent with the lack of suppression for the hydrophilic non-polymer molecules observed here. Furthermore, the faster suppression observed for PPG can be ascribed to the introduction of more hydrophobic propylene oxide (PO) units. This is also consistent with the earlier discussion on the S-shaped current transients in potentiostatic treatment, where the adsorption rate is facilitated by some hydrophobic attractive interaction between adsorbed molecules on surface and dissolved molecules in electrolyte. When 500 ppm PEG-PPG-PEG are added into the electrolyte, similar suppression behavior as ETT is observed.

To further investigate the suppression effect of PEG-PPG-PEG on Sn deposition, similar potentiostatic pretreatments as in Fig. 5 are conducted. The results are presented in Fig. S-4 in Supporting Information. Similar trends in suppression behavior are observed, namely, the current decays during the potentiostatic treatment and the rate of this decay is also potential dependent. However, the current decay is much faster than the cases with ETT in Fig. 5(a), suggesting a higher adsorption rate constant for PEG-PPG-PEG at the same potential. This faster adsorption is also manifested by the facts that 30 sec pretreatment at -0.45 V is sufficient to immediately suppress the Sn deposition in CV study and that the pretreatment at OCP also causes sooner and stronger suppression than the same treatment with ETT, both shown in Fig. S-4(b).

Chronopotentiometry is also carried out to confirm the findings. In this set of studies, galvanostatic plating is carried out at a current density of -10 mA/cm^2 and a rotation rate of 1000 rpm with a lower dose of 100 ppm of PEG-PPG-PEG or ETT being injected in the vicinity of RDE. The potential transients are shown in Fig. 8. Upon the additive injection at 100 s, a larger potential drop is observed for PEG-PPG-PEG than ETT, which suggests a stronger suppression effect for the PEG-PPG-PEG copolymer than ETT. In other words, thermodynamically speaking, it is more difficult for the electron to transfer across the adsorbed PEG-PPG-PEG layer than the ETT layer. At the same time, it takes around 30 s for the potential to drop in ETT case whilst it only takes less than 10 s for PEG-PPG-PEG. This confirms that the adsorption process of PEG-PPG-PEG is faster than ETT. Studies showed that PEG with higher molecular weights often inhibits Cu deposition more strongly [52–54]. However, the hydrophobicity of molecule plays an even more important role [55]. In this study, despite of a higher molecular weight of ETT (7,200)

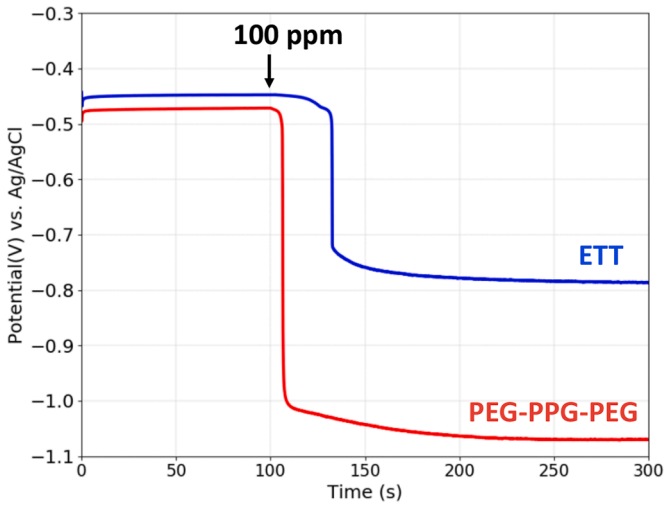

Fig. 8. Potential transients upon injection of 100 ppm of ETT or PEG-PPG-PEG co-polymer during galvanostatic Sn deposition at -10 mA/cm^2 on RDE at a rotation rate of 1000 rpm.

than PEG-PPG-PEG (4,400), the detailed EO/PO ratio and therefore the hydrophobicity can be different. Furthermore, the presence of ethylenediamine motif in ETT also improves its overall hydrophilicity. The PEG-PPG-PEG co-polymer used here has a much lower cloud point than the ETT (14°C vs. 43°C), indicating a much higher hydrophobicity. This is believed to result in the faster and stronger suppression observed in this study. Again, this appears to be consistent with the S-shaped current transients, where the adsorption is facilitated by the hydrophobic attraction between adsorbate on surface and additive molecules in electrolyte.

3. Conclusion

Sn electrodeposition is suppressed within a certain negative potential range in the presence of ETT. A potential dependent adsorption mechanism is proposed and examined through a systematic study on the effects of ETT concentration, rotation rate, and scan rate. The adsorption rate was found to depend not only on the empty surface fraction but also on the occupied fraction, suggesting an attractive interaction between the molecules adsorbed on surface and molecules dissolved in electrolyte. While a higher ETT concentration facilitates such adsorption, a higher rotation rate or stronger agitation results in adsorbate detachment upon hydrodynamic shear. The effects of the functional groups of ETT are studied using various additives with different similarities. The highly hydrophilic ethylenediamine derivatives do not show any suppression behavior, whilst the poly(alkylene glycol) polymers show various degrees of suppression. Among them, the PEG-PPG-PEG triblock co-polymer shows faster adsorption and stronger suppression effect than ETT, probably attributed to a higher hydrophobicity.

CRediT authorship contribution statement

Y. Hu: Data curation, Investigation, Formal analysis, Writing – original draft, Writing – review & editing. **K. Ahammed:** Data curation, Investigation. **Q. Liu:** Data curation, Investigation. **R. Williams:** Data curation, Investigation. **Q. Huang:** Conceptualization, Formal analysis, Writing – original draft, Writing – review & editing.

Declaration of Competing Interest

The authors declare that they have no known competing financial interests or personal relationships that could have appeared to influence the work reported in this paper.

Acknowledgements

National Science Foundation is acknowledged for support through grants 1921840 and 1662332. RW acknowledges NSF REU site grant 1851974 for the summer research program. YH thanks the Graduate Council at University of Alabama for a fellowship support.

Supplementary materials

Supplementary material associated with this article can be found, in the online version, at doi:10.1016/j.electacta.2022.140476.

References

[1] R. Sekar, C. Eagammai, S. Jayakrishnan, Effect of additives on electrodeposition of tin and its structural and corrosion behaviour, J. Appl. Electrochem. 40 (1) (2010) 49–57.
[2] L. Anicai, A. Petica, S. Costovici, P. Prioteasa, T. Visan, Electrodeposition of Sn and NiSn alloys coatings using choline chloride based ionic liquids—Evaluation of corrosion behavior, Electrochim. Acta 114 (2013) 868–877.
[3] F.A. Lowenheim, J. Davis, Modern electroplating, J. Electrochem. Soc. 121 (12) (1974) 397C.
[4] M. Carano, Tin plating, Plat. Surf. Finish. 87 (8) (2000) 64–65.
[5] A. Brenner, Electrodeposition of Alloys, 2 volumes, Academic Press, 1963.
[6] Y. Nakamura, N. Kaneko, M. Nakamura, H. Nezu, Synergistic effects of benzalacetone and benzophenone on the electrocrystallization of tin from acid stannous sulphate solutions, J. Appl. Electrochem. 24 (5) (1994) 404–410.
[7] Y. Nakamura, N. Kaneko, H. Nezu, Surface morphology and crystal orientation of electrodeposited tin from acid stannous sulphate solutions containing various additives, J. Appl. Electrochem. 24 (6) (1994) 569–574.
[8] I.S. Zavarine, O. Khaselev, Y. Zhang, Spectroelectrochemical study of the effect of organic additives on the electrodeposition of tin, J. Electrochem. Soc. 150 (4) (2003) C202.
[9] A. Aragon, M. Figueroa, R. Gana, J. Zagal, Effect of a polyethoxylate surfactant on the electrodeposition of tin, J. Appl. Electrochem. 22 (6) (1992) 558–562.
[10] J.Y. Lee, J.W. Kim, B.Y. Chang, H.T. Kim, S.M. Park, Effects of ethoxylated α-naphtholsulfonic acid on tin electroplating at iron electrodes, J. Electrochem. Soc. 151 (5) (2004) C333.
[11] G. Tzeng, S. Lin, Y. Wang, C. Wan, Effects of additives on the electrodeposition of tin from an acidic Sn (II) bath, J. Appl. Electrochem. 26 (4) (1996) 419–423.
[12] C. Low, F. Walsh, The influence of a perfluorinated cationic surfactant on the electrodeposition of tin from a methanesulfonic acid bath, J. Electroanal. Chem. 615 (2) (2008) 91–102.
[13] S. Wen, J.A. Szpunar, Nucleation and growth of tin on low carbon steel, Electrochim. Acta 50 (12) (2005) 2393–2399.
[14] F. Barry, V. Cunnane, Synergistic effects of organic additives on the discharge, nucleation and growth mechanisms of tin at polycrystalline copper electrodes, J. Electroanal. Chem. 537 (1-2) (2002) 151–163.
[15] F. Walsh, C. Low, A review of developments in the electrodeposition of tin, Surf. Coat. Technol. 288 (2016) 79–94.
[16] N. Kaneko, N. Shinohara, H. Nezu, Effects of aromatic carbonyl compounds on the surface morphology and crystal orientation of electrodeposited tin from acid stannous sulfate solutions, Electrochim. Acta 37 (13) (1992) 2403–2409.
[17] G. Medvedev, N. Makrushin, Electrodeposition of tin from sulfate electrolyte with organic additives, Russ. J. Appl. Chem. 74 (11) (2001) 1842–1845.
[18] F. Wang, P. Zeng, Y. Wang, X. Ren, H. Xiao, W. Zhu, High-speed and high-quality TSV filling with the direct ultrasonic agitation for copper electrodeposition, Microelectron. Eng. 180 (2017) 30–34.
[19] K. Kondo, C. Funahashi, Y. Miyake, Y. Takeno, T. Hayashi, M. Yokoi, N. Okamoto, T. Saito, Five-minute TSV copper electrodeposition, J. Electrochem. Soc. 161 (14) (2014) D791.
[20] H. Xiao, H. He, X. Ren, P. Zeng, F. Wang, Numerical modeling and experimental verification of copper electrodeposition for through silicon via (TSV) with additives, Microelectron. Eng. 170 (2017) 54–58.
[21] C. Okoro, R. Labie, K. Vanstreels, A. Franquet, M. Gonzalez, B. Vandevelde, E. Beyne, D. Vandepitte, B. Verlinden, Impact of the electrodeposition chemistry used for TSV filling on the microstructural and thermo-mechanical response of Cu, J. Mater. Sci. 46 (11) (2011) 3868–3882.
[22] O. Lühn, A. Radisic, P. Vereecken, C. Van Hoof, W. Ruythooren, J.P. Celis, Changing superfilling mode for copper electrodeposition in blind holes from differential inhibition to differential acceleration, Electrochem. Solid State Lett. 12 (5) (2009) D39.
[23] A. Radisic, O. Lühn, H. Philipsen, Z. El-Mekki, M. Honore, S. Rodet, S. Armini, C. Drijbooms, H. Bender, W. Ruythooren, Copper plating for 3D interconnects, Microelectron. Eng. 88 (5) (2011) 701–704.
[24] M. Hayase, K. Otsubo, Copper deep via filling with selective accelerator deactivation by a reverse pulse, J. Electrochem. Soc. 157 (12) (2010) D628.
[25] S. Wang, S.R. Lee, Fast copper plating process for through silicon via (TSV) filling, in: Proceedings of the ASME International Mechanical Engineering Congress and Exposition, 2011, pp. 855–863.

[26] T. Moffat, D. Josell, Extreme bottom-up superfilling of through-silicon-vias by damascene processing: suppressor disruption, positive feedback and turing patterns, J. Electrochem. Soc. 159 (4) (2012) D208.
[27] M. Takeuchi, K. Kondo, H. Kuri, M. Bunya, N. Okamoto, T. Saito, Single diallylamine-type copolymer additive which perfectly bottom-up fills Cu electrodeposition, J. Electrochem. Soc. 159 (4) (2012) D230.
[28] D. Josell, D. Wheeler, T. Moffat, Modeling extreme bottom-up filling of through silicon vias, J. Electrochem. Soc. 159 (10) (2012) D570–D576.
[29] D. Wheeler, T.P. Moffat, D. Josell, Spatial-temporal modeling of extreme bottom-up filling of through-silicon-vias, J. Electrochem. Soc. 160 (12) (2013) D3260.
[30] L. Yang, A. Radisic, J. Deconinck, P. Vereecken, The limitation and optimization of bottom-up growth mode in through silicon via electroplating, J. Electrochem. Soc. 162 (14) (2015) D599.
[31] M. Takeuchi, Y. Anami, Y. Yamada, M. Bunya, S. Okada, N. Okamoto, T. Saito, M. Yokoi, K. Kondo, Effect of counter ions in a diallylamine-type copolymer additive on via-filling by copper electrodeposition, Electrochemistry 82 (6) (2014) 430–437.
[32] Y. Yamada, K. Kondo, M. Takeuchi, N. Okamoto, T. Saito, M. Bunya, Y. Yokoi, Effect of basicity of amino group at side chain in diallylamine-type copolymer additive on via-filling by copper electrodeposition, ECS Trans. 58 (17) (2014) 97.
[33] H. Yang, A. Dianat, M. Bobeth, G. Cuniberti, Copper electroplating with polyethylene glycol, J. Electrochem. Soc. 164 (4) (2017) D196.
[34] D. Josell, T.P. Moffat, Superconformal copper deposition in through silicon vias by suppression-breakdown, J. Electrochem. Soc. 165 (2) (2018) D23.
[35] S.H. Kim, H.J. Lee, T.M. Braun, T.P. Moffat, D. Josell, Effect of chloride on microstructure in Cu filled microscale through silicon vias, J. Electrochem. Soc. 168 (11) (2021) 112501.
[36] T. Moffat, D. Josell, Extreme bottom-up superfilling of through-silicon-vias by damascene processing: suppressor disruption, positive feedback and turing patterns, J. Electrochem. Soc. 159 (4) (2012) D208–D216.
[37] D. Josell, T. Moffat, Superconformal copper deposition in through silicon vias by suppression-breakdown, J. Electrochem. Soc. 165 (2) (2018) D23–D30.
[38] M.L. Walker, L.J. Richter, T.P. Moffat, *In situ* ellipsometric study of PEG/ Cl-coadsorption on Cu, Ag, and Au, J. Electrochem. Soc. 152 (6) (2005) C403.
[39] Z.V. Feng, X. Li, A.A. Gewirth, Inhibition due to the interaction of polyethylene glycol, chloride, and copper in plating baths: a surface-enhanced Raman study, J. Phys. Chem. B 107 (35) (2003) 9415–9423.
[40] G.-K. Liu, S. Zou, D. Josell, L.J. Richter, T.P. Moffat, SEIRAS study of chloride-mediated polyether adsorption on Cu, J. Phys. Chem. C 122 (38) (2018) 21933–21951.
[41] D. Josell, T. Moffat, Extreme bottom-up filling of through silicon vias and damascene trenches with gold in a sulfite electrolyte, J. Electrochem. Soc. 160 (12) (2013) D3035–D3039.
[42] D. Josell, T.P. Moffat, Superconformal bottom-up gold deposition in high aspect ratio through silicon vias, J. Electrochem. Soc. 164 (6) (2017) D327.
[43] D. Josell, T.P. Moffat, Bottom-up electrodeposition of zinc in through silicon vias, J. Electrochem. Soc. 162 (3) (2015) D129.
[44] S.K. Kim, J.E. Bonevich, D. Josell, T.P. Moffat, Electrodeposition of Ni in submicrometer trenches, J. Electrochem. Soc. 154 (9) (2007) D443.
[45] D. Josell, T.P. Moffat, Superconformal bottom-up nickel deposition in high aspect ratio through silicon vias, J. Electrochem. Soc. 163 (7) (2016) D322–D331.
[46] D. Josell, M. Silva, T.P. Moffat, Superconformal bottom-up cobalt deposition in high aspect ratio through silicon vias, J. Electrochem. Soc. 163 (14) (2016) D809–D817.
[47] W.M. Haynes, D.R. Lide, T.J. Bruno, CRC Handbook of Chemistry and Physics, CRC press, 2016.
[48] T.M. Braun, D. Josell, M. Silva, J. Kildon, T. Moffat, Effect of chloride concentration on copper deposition in through silicon vias, J. Electrochem. Soc. 166 (1) (2019) D3259.
[49] T. Braun, D. Josell, T. Moffat, Microelectrode studies of S-NDR copper electrodeposition: potentiodynamic and galvanodynamic measurements and simulations, J. Electrochem. Soc. 167 (8) (2020), 082509.
[50] D. Josell, L. Menk, A. Hollowell, M. Blain, T. Moffat, Bottom-up copper filling of millimeter size through silicon vias, J. Electrochem. Soc. 166 (1) (2019) D3254.
[51] L. Menk, D. Josell, T. Moffat, E. Baca, M. Blain, A. Smith, J. Dominguez, J. McClain, P. Yeh, A. Hollowell, Bottom-up copper filling of large scale through silicon vias for MEMS technology, J. Electrochem. Soc. 166 (1) (2018) D3066.
[52] W.P. Dow, M.Y. Yen, W.B. Lin, S.W. Ho, Influence of molecular weight of polyethylene glycol on microvia filling by copper electroplating, J. Electrochem. Soc. 152 (11) (2005) C769.
[53] L. Yin, Z. Liu, Z. Yang, Z. Wang, S. Shingubara, Effect of PEG molecular weight on bottom-up filling of copper electrodeposition for PCB interconnects, Trans. IMF 88 (3) (2010) 149–153.
[54] S.L. Ko, J.Y. Lin, Y.Y. Wang, C.C. Wan, Effect of the molecular weight of polyethylene glycol as single additive in copper deposition for interconnect metallization, Thin Solid Films 516 (15) (2008) 5046–5051.
[55] J.W. Gallaway, A.C. West, PEG, PPG, and their triblock copolymers as suppressors in copper electroplating, J. Electrochem. Soc. 155 (10) (2008) D632–D639.